Predicting and evaluating side effects of radiotherapy in cervical cancer

Corbeau, A.

Chapter 7

Changes in bone marrow fat fraction and immune cell counts in women with cervical cancer treated with primary chemoradiotherapy

Anouk Corbeau, Eleftheria Astreinidou, Sander C. Kuipers, Piotr A. Wielopolski, Wendy Visser, Jan Willem M. Mens, Henrike Westerveld, Mila Donker, Laura A. Velema, Judith R. Kroep, Ingrid A. Boere, Marij J.P. Welters, Sjoerd H. van der Burg, Mischa S. Hoogeman, Hein Putter, Jeremy Godart, Uulke A. van der Heide, Carien L. Creutzberg, Remi A. Nout, Stephanie M. de Boer

Radiotherapy & Oncology, 2025, 211:111089.

ABSTRACT

Introduction

Hematologic toxicity (HT) is a common effect of chemoradiotherapy in primary locally advanced cervical cancer (LACC) and related to bone marrow (BM) fat increase. However, longitudinal effects and dose-relationships are unknown. In this study, pre- and post-treatment BM fat fraction and blood immune cell counts were evaluated in women with primary LACC undergoing BM sparing chemoradiotherapy.

Materials and Methods

Water-fat MRI scans and blood samples were obtained at baseline, during, and at 3 and 12 months (post-)treatment. The mean proton density fat fraction (PDFF) [%] was calculated for each vertebra, categorized into a no (<1 Gy), low (1-5 Gy), and high (>5 Gy) dose group, and the pelvic bones. Associations between PDFF and dose, immune cells, and patient characteristics were assessed with linear mixed models.

Results

Eighteen women were included. Vertebral PDFF in the no dose group remained unchanged, whereas the low and high dose group showed an increase of 24-35 PDFF% during treatment. PDFF in the low dose group recovered slightly but remained elevated up to 12 months post-treatment. Mean dose to pelvic subregions was ≥18.8 Gy and PDFF increase was 12-29 PDFF%. Only the lower pelvic PDFF recovered to baseline. Blood immune cell decline lasted up to 12 months post-treatment and was correlated with higher mean vertebral PDFF.

Conclusion

Vertebral fat fraction increased during treatment for dose >1 Gy, without post-treatment recovery for dose >5 Gy. Immunosuppression persisted up to 12 months post-treatment and was related to a higher mean vertebral PDFF. 5 Gy might be relevant for BM damage, but this threshold should be validated.

INTRODUCTION

Hematologic toxicity (HT) is a common side effect in women with primary locally advanced cervical cancer (LACC) treated with platinum-based chemoradiotherapy followed by image-guided brachytherapy. The incidence of moderate (grade 2) acute (within 3 months after treatment) HT ranges from 67.5%-82.31% [1-5] and of severe (grade 3) acute HT between 45%-53.85% [4-7]. Even with bone marrow sparing radiotherapy, 50%-83% of the women develop grade 2 acute HT [1, 4] and 32.3%-37% develop grade 3 acute HT [4, 7]. Lymphopenia is the most common effect of radiotherapy [8]. Multiple studies found associations between lymphopenia and poorer long-term outcomes after chemoradiation [8-10]. The biological mechanism behind this relationship is not yet known, but since lymphocytes are instrumental for an effective antitumor response, lymphopenia might inhibit this process [11, 12]. Additionally, immunotherapy combined with chemoradiotherapy as a new standard of care for high risk LACC is gaining interest [13]. Since lymphocytes are key to the clinical impact of immunotherapy, lymphopenia may compromise its efficacy [14-16].

The red bone marrow, which is mostly located in the pelvic bones and vertebrae [17, 18], serves as a principal home for the hematopoietic stem cells (HSCs) and is actively involved in generating hematopoietic cells [19, 20]. Chemoradiotherapy can injure or directly deplete these HSCs, damage the HSC niche, or injure regulatory cells and therefore cause HT [17, 21-23]. In mice, adipocytes populate the bone marrow between two and four weeks, and perhaps even earlier, as a response to irradiation [24, 25]. Several studies used water-fat MRI scans to detect an increase in bone marrow fat fraction due to chemoradiation in patients with pelvic or gynecological cancers [26-30] and this was correlated with a decrease in circulating blood cells [26, 29, 30]. However, these studies had a limited follow-up time, included a heterogeneous patient cohort, or did not evaluate bone marrow outside the radiation field, prohibiting the evaluation of radiotherapy-specific changes.

The aim of this study was to evaluate longitudinal changes in bone marrow fat fraction and blood immune cells in women with locally advanced cervical cancer treated with primary bone marrow sparing chemoradiotherapy. We evaluated bone marrow fat fraction before, during, and up to 12 months after treatment in the vertebral column and (subregions of the) pelvic bones and linked this to peripheral immune cell counts.

METHODS

Study design and patients

Women with locally advanced cervical cancer (LACC) treated with primary chemoradiotherapy using bone marrow sparing volumetric-modulated arc therapy (VMAT) and weekly cisplatin, followed by MR-guided brachytherapy, in the prospective, multicenter PROTECT study (NCT05406856) were analyzed for this study [31]. Participants were recruited between May 2022 and September 2023 in Leiden University Medical Center (LUMC) and Erasmus Medical Center (EMC) in the Netherlands. The study was approved by the Medical Ethics Review Committee Leiden The Hague Delft and Medical Ethics Review Committee Erasmus Medical Center. All participants provided informed consent.

Treatment

All women received bone marrow sparing VMAT with a total dose of 45 Gy in 25 daily fractions in five weeks, using a library-of-plans technique, according to the EMBRACE-II guidelines [32]. Based on bladder filling observed on the planning CT scans acquired with both full and empty bladder, one to three treatment plans were generated to cover the motion of the uterus. The most appropriate treatment plan from this library-of-plans was selected for treatment each day using cone beam CT. Involved nodes were boosted using a simultaneous integrated boost (SIB) to reach a total equivalent dose of 60 Gy $EQD2_{10}$. The whole pelvic bones were delineated as a substitute for the bone marrow on the planning CT-scan extending from 24–25 mm above the planning target volume (PTV) to the inferior border of the ischial tuberosities [33]. The bone marrow was spared by inducing planning aims of V_{10Gy}<90%, V_{20Gy}<65%, and V_{40Gy}<15–20% [34, 35]. Concurrent chemotherapy consisted of weekly cisplatin (40 mg/m^2) for five weeks. MR-guided brachytherapy was performed using 90–95 Gy ($EQD2_{10}$ D90) to the high-risk-clinical target volume (CTV-HR) [32].

Water-fat MRI imaging

Patients underwent water-fat MRI before the start of treatment, for brachytherapy planning (after external beam radiation therapy (EBRT)), and 3 and 12 months after the end of treatment. The water-fat MRI sequences used were multi-point quantitative Dixon (mDixon Quant) from Philips in LUMC and iterative decomposition of water and fat

with echo asymmetry and least squares estimation (IDEAL IQ) from General Electric (GE) HealthCare in EMC. Both 1.5-T and 3.0-T scanners were used. The MRI scanners, scanning procedure, and scanner settings used were described in a previously reported validation study [36]. Proton density fat fraction (PDFF) maps were reconstructed with the vendors' commercial software and imported into treatment planning system Raystation (version 2023B, RaySearch Laboratories, Sweden).

PDFF map analysis

The process for placing regions-of-interest (ROIs) in the vertebrae and pelvic bones is visualized in Figure 1. Box-shaped ROIs were placed in the middle of cervical (C) vertebra 7 to sacral (S) vertebra 2. The outer contour of three subregions of the pelvic bones, consisting of the ilium, lower pelvis, and lumbosacral spine (excluding the cauda equina), was delineated and contracted by 4 mm to exclude the bone cortex [33]. The whole pelvic bone ROI included all three subregions. The mean PDFF was calculated over all voxels per ROI.

Dosimetric evaluation

The baseline reconstructed PDFF map was registered to the planning CT-scan. The box-shaped ROIs from the vertebrae were transferred to the planning CT-scan and adjusted manually to be positioned in the middle of each vertebra. For the pelvic bones, the whole pelvic bones ROI on the planning CT-scan, used for treatment planning, was divided into the three subregions ilium, lower pelvis, and lumbosacral spine [33]. The D_{mean} [Gy] per vertebra and the D_{mean}, [Gy] and absolute [cc] and relative [%] V_{10Gy}, V_{20Gy}, and V_{40Gy} for the whole pelvic bones and per pelvic bone subregion were determined based on the full bladder treatment plan. This plan is generally the most frequently selected during treatment, as patients follow a drinking protocol with the aim of being treated with a full bladder, in accordance with the EMBRACE-II guidelines [32]. Pelvic bone dose from brachytherapy was considered negligible.

Laboratory blood tests and hematologic toxicity grading

Blood cell analysis was carried out at the diagnostic hematology laboratory, as part of routine full blood cell counts, at baseline, before the fourth chemotherapy administration, and 3 and 12 months after treatment. Hematologic toxicity was graded using Common Terminology Criteria Adverse Events (CTCAE) v5.0 [37].

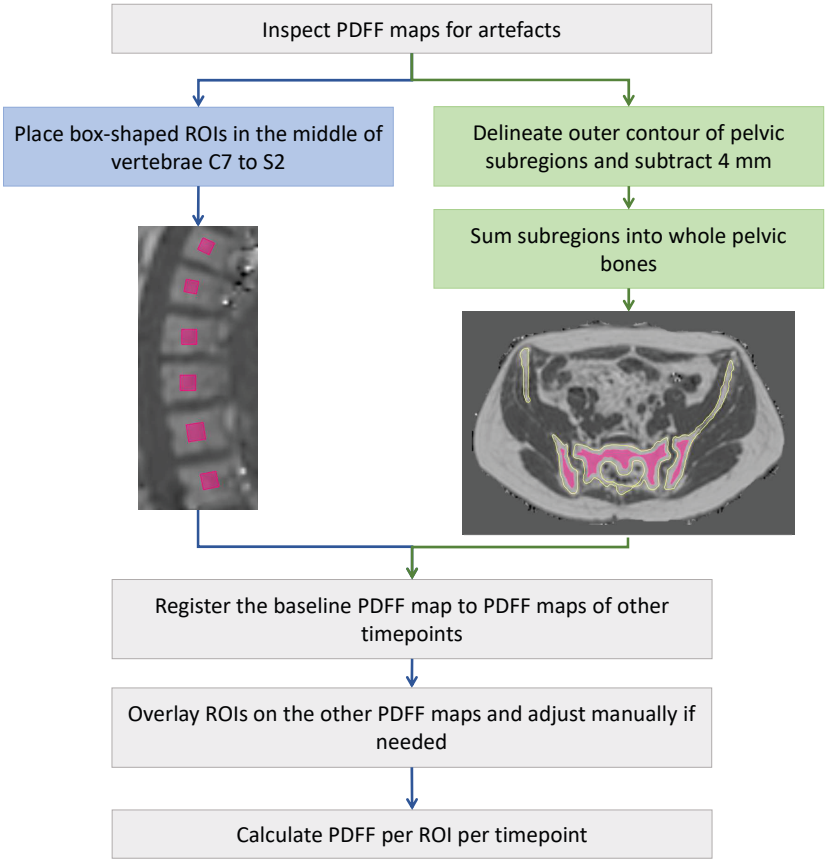

Figure 1: *Process of delineating the vertebrae (the left track in blue) and the pelvic bones (the right track in green) on the proton density fat fraction (PDFF) maps. The ROI per vertebra and of the whole pelvic bones are indicated with pink in the left and right PDFF map, respectively. ROIs = regions-of-interest, C = cervical, S = sacral.*

Statistical analysis

Vertebrae were categorized into three groups based on EBRT dose. The no, low, and high dose group included vertebrae having respectively a D_{mean} <1 Gy , 1–5 Gy, and >5 Gy. The threshold of 5 Gy was chosen to include vertebrae at the field edge and because previous studies have demonstrated that this dose was associated with HT and a significant reduction in bone marrow activity [38, 39]. Linear mixed-effects models were utilized to evaluate PDFF and immune cell changes in the blood over time and to assess the association between PDFF and immune cell counts. For PDFF, age and D_{mean} were normalized based on the mean of the evaluated women. Body mass index

(BMI), smoking status, and the interaction between dose group (vertebrae) or centered D_{mean} (whole pelvic bones or subregion of the pelvic bones) and timepoint and between centered age and timepoint were included as fixed effects. For immune cell changes, timepoint was included as fixed effect. For the associations between PDFF and blood immune cell counts, age, BMI, smoking, and mean PDFF of the vertebral column were included as fixed effects. In all models, the patient's identifier was included as random effect. A p-value <0.05 was considered significant. Changes in PDFF greater than 10% were considered substantial, as these exceed the range of measurement variability in water-fat MRI validation studies [36, 40-43]. Statistical analyses were performed with R (v4.3.1).

RESULTS

In total, 20 women were included in the PROTECT study. Two withdrew informed consent before the start of the treatment, resulting in 18 women eligible for analysis. Table 1 presents the patient characteristics. Eleven women finished five cycles of cisplatin chemotherapy, five patients received four cycles of chemotherapy due to cisplatin-related side effects including tinnitus, hyponatremia, thrombopenia, elevated liver enzymes, and hematologic toxicity (HT) (thrombopenia, anemia, leukopenia, lymphopenia), and two patients were referred for hyperthermia due to kidney insufficiency or elevated liver enzymes after one or two chemotherapy cycles. All patients underwent brachytherapy. Table S1 shows the EBRT dosimetric parameters of the pelvic bones. Bone marrow sparing constraints were fulfilled in all women except for one woman with V_{10Gy}, V_{20Gy}, and V_{40Gy} of 90.1%, 72.9%, and 15.8%, respectively, and for two women with a V_{20Gy} of 65.9% and 67.2%. Out of 18 women, 11 completed all MRI scans, 12 all lymphocyte counts and 14 all neutrophil and leukocyte counts. Missing data post-treatment were due to patient refusal (n = 2) or disease progression (n = 1 after treatment, n = 1 at 3 months after treatment). Other scans and blood samples were missing due to technical or logistical issues. An overview of the data available per timepoint is provided in Table S2.

Table 1: *Patient characteristics of the 18 evaluated women, treated with primary chemoradiotherapy using bone marrow sparing volumetric-modulated arc therapy and weekly cisplatin, followed by brachytherapy. BMI = body mass index, FIGO = International Federation of Gynecology and Obstetrics, PAO = para-aortic.*

Characteristic	**mean (sd) or n [%]**
Age [years]	52.3 (15.0)
BMI [kg/m^2]	27.4 (5.3)
Smoking	
yes	2 [11.1%]
former	4 [22.2%]
no	12 [66.7%]
Tumor type	
squamous	13 [76.5%]
adeno	4 [23.5%]
unknown	1
FIGO stage (2018)	
IIB	5 [27.8%]
IIIB	1 [5.6%]
IIIC1	12 [66.7%]
No. of chemotherapy cycles finished	
1	1 [5.6%]
2	1 [5.6%]
4	5 [27.8%]
5	11 [61.1%]
PAO lymph node irradiation	
yes	10 [55.6%]
no	8 [44.4%]
Blood transfusions during treatment	
erythrocytes	1 [5.6%]
thrombocytes	1 [5.6%]
erythrocytes and thrombocytes	1 [5.6%]
none	15 [83.3%]

Figure 2 shows mean PDFF changes per vertebra for all evaluated patients. The vertebrae cervical (C) 7 – thoracic (T) 11 received a mean dose ≤0.5 Gy and PDFF did not increase substantially due to chemoradiotherapy, as the maximum PDFF increase was 9.8 PDFF% (for T11). T12 received a mean dose of 4.2 Gy and mean PDFF increased from 35.8% to 56.4% (+20.6 ΔPDFF%) due to chemoradiotherapy, followed by an average decrease to 46.8% (-9.6 ΔPDFF%) and 48.1% (-8.3 ΔPDFF%) at 3 and 12 months after treatment. The mean PDFF of lumbar (L) 1, with a mean dose of 12 Gy, increased from 36.8% to 69.6% (+32.8 ΔPDFF%) and showed less recovery after EBRT, as mean PDFF were 64.2%

(-5.5 ΔPDFF%) and 61.5% (-8.1 ΔPDFF%) at 3 and 12 months post-treatment. Vertebrae L2 – sacral (S) 2 received mean doses ≥23 Gy, resulting in mean PDFF increases of ≥22.4 PDFF% without recovery up to 12 months after treatment.

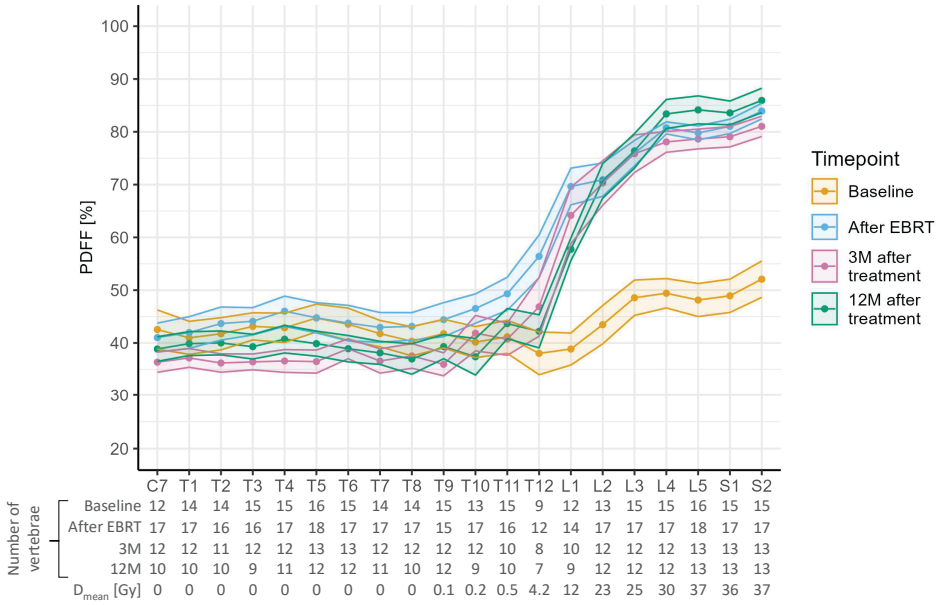

***Figure 2**: Mean proton density fat fraction (PDFF) [%] and corresponding 95% confidence intervals per vertebra per timepoint of 18 women with locally advanced cervical cancer treated with bone marrow sparing chemoradiotherapy with volumetric-modulated arc therapy. Per timepoint and vertebra, the number of available vertebrae and the mean D_{mean} [Gy] are indicated in the table below the figure. EBRT = external beam radiation therapy, M = months, C = cervical, T = thoracic, L = lumbar, S = sacral.*

Figure 3 visualizes PDFF changes per vertebral dose group for all 18 evaluated patients. The results from the linear mixed-effects model are shown in Table S3. Timepoint, dose group, and age were significantly associated with PDFF. Mean PDFF at baseline ranged between 39.2% and 45.8% for the three dose groups. Mean PDFF did not change substantially between timepoints in vertebrae receiving no dose. In vertebrae receiving a low or high dose, mean PDFF increased from 39.2% to 63.0% (+23.8 ΔPDFF%) or 45.8% to 80.4% (+34.7 ΔPDFF%) between baseline and after EBRT, respectively. In the low dose group, mean PDFF decreased from 63.0% to 49.7% (-13.3 ΔPDFF%) and 56.3% (-6.7 ΔPDFF%) at 3 and 12 months post-treatment but remained elevated compared to baseline. As post-treatment PDFF changes ranged between -1.9 and 1.2 PDFF%, no

recovery was detected in the high dose group up to 12 months post-treatment. The effect of age on PDFF varied among timepoints, as age had the largest impact on baseline PDFF, resulting in an increase of 0.8 PDFF% per life year. BMI and smoking were not correlated with PDFF.

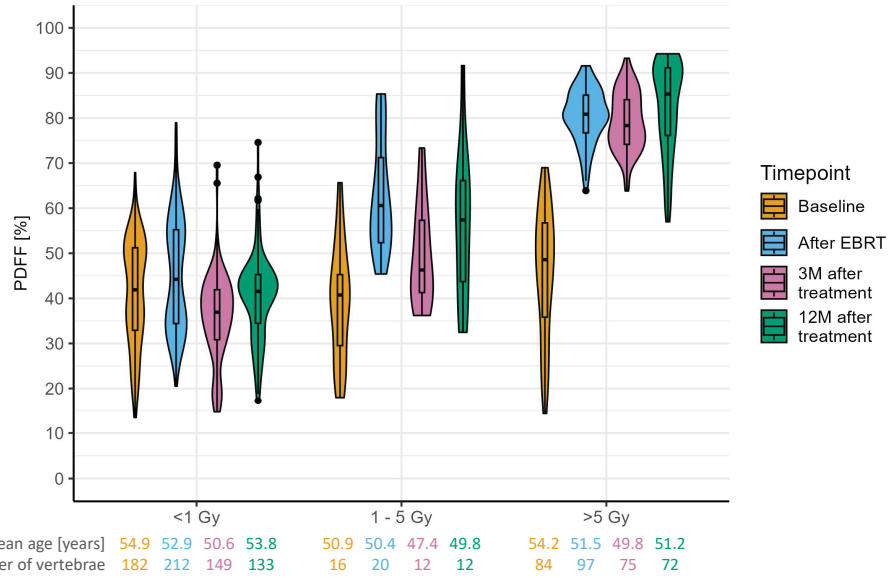

Figure 3: *Median, quartiles, and range of proton density fat fraction (PDFF) [%] for the vertebrae of 18 women with locally advanced cervical cancer treated with bone marrow sparing chemoradiotherapy with volumetric-modulated arc therapy. Vertebrae were subdivided based on D_{mean} per vertebra from external beam radiation therapy (EBRT) into no (<1 Gy), low (1 – 5 Gy), and high dose (>5 Gy). Per timepoint and dose group, the mean age of the women and the number of vertebrae available for analysis are indicated in the table below the figure. M = month.*

Regarding the whole pelvic bones, the PDFF increased, on average, from 62.6% to 84.0% (+21.4 ΔPDFF%) due to chemoradiotherapy without post-treatment recovery, as PDFF at 3 and 12 months after treatment were 78.1% and 79.8% (Figure 4, Table S4). Timepoint and age were significantly associated with whole pelvic bones PDFF. A higher age at baseline was significantly associated with a higher PDFF (+0.43 PDFF% per life year), but this relationship was not observed at the other timepoints. D_{mean}, BMI, and smoking were not correlated with PDFF.

For the pelvic subregions, the PDFF increased on average from 53.8 to 82.4% (+28.6 ΔPDFF%), from 74.0 to 85.9% (+11.9 ΔPDFF%), and 55.2 to 81.7% (+26.5 ΔPDFF%)

for the ilium, lower pelvis, and sacrum, respectively (Figure 4, Table S5). None of the subregions showed a post-treatment PDFF recovery >10 PDFF%. However, the lower pelvis PDFF returned to baseline levels with a mean PDFF of 79.3% and 80.1% at 3 and 12 months, respectively. D_{mean} was related to PDFF of the ilium at 12 months after treatment (+4.09 PDFF% per Gy), but not with other timepoints or pelvic subregions. Age contributed to baseline PDFF of the ilium and sacrum with +0.57 and +0.82 PDFF% per life year, respectively. BMI and smoking were not correlated with PDFF.

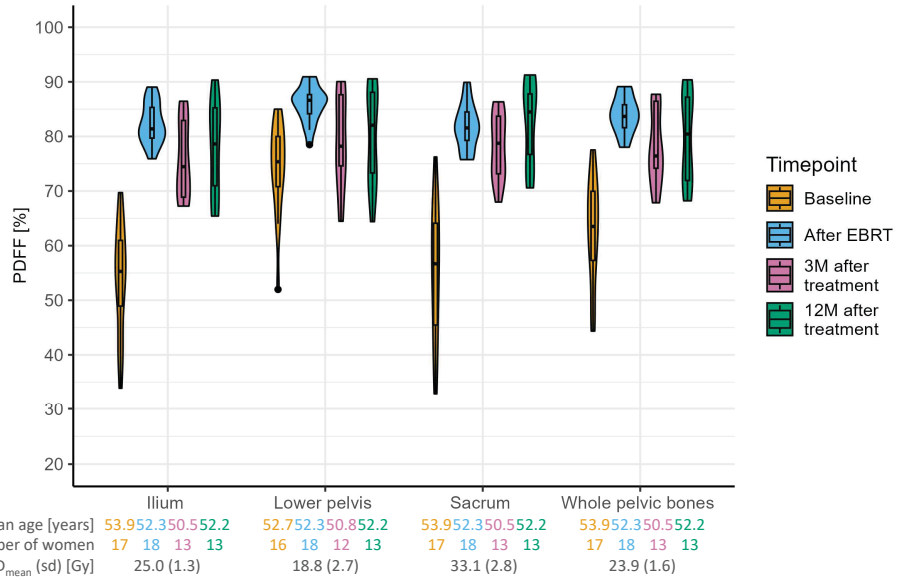

***Figure 4**: Median, quartiles, and range of proton density fat fraction (PDFF) [%] for the subregions of the pelvic bones of 18 patients with locally advanced cervical cancer treated with bone marrow sparing chemoradiotherapy with volumetric-modulated arc therapy. Per pelvic subregion, the mean age and the number of pelvic bone structures available per timepoint and the mean D_{mean} (sd) [Gy] are indicated in the table below the figure. EBRT = external beam radiation therapy, M = months.*

Figure 5 shows that the number of circulating lymphocytes per patient decreased with increasing mean PDFF of the vertebral column. All women developed grade ≥2 lymphopenia during treatment. Similarly, a relationship between mean PDFF of the vertebral column and the number of circulating leukocytes and neutrophils was observed (Figure S1). Circulating immune cell counts did not recover to baseline level during the 12 months post-treatment (Figure S2, all $p<0.001$). A lower mean PDFF of the vertebral column and higher age significantly contributed to an increasing number of lymphocytes, whereas BMI and smoking did not (Table S6A). Similar relationships were

observed between age and the number of circulating leukocytes (Figure S1 and Table S6B). However, for the circulating neutrophil count, only the mean PDFF of the vertebral column was significantly associated (Figure S1 and Table S6C).

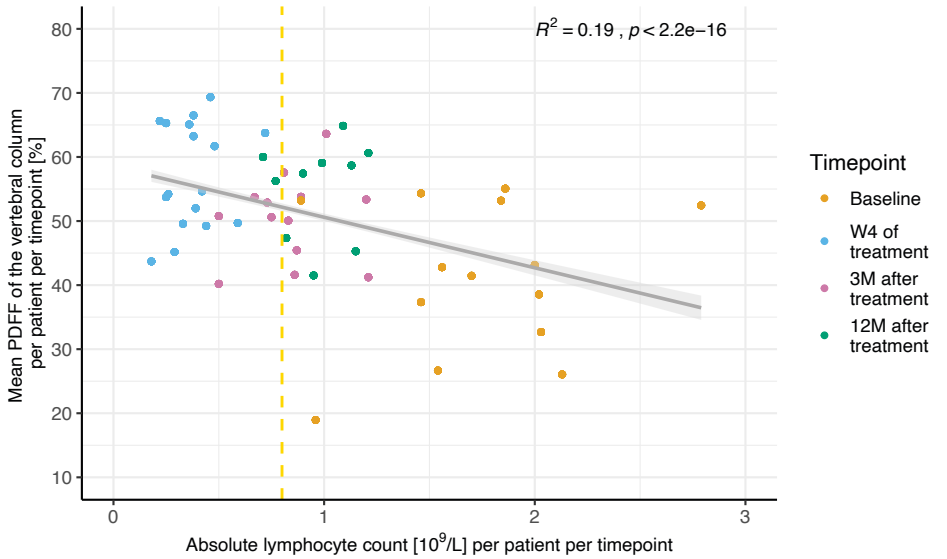

Figure 5: *Mean proton density fat fraction (PDFF) [%] of the vertebral column compared with the number of lymphocytes [10^9/L] per patient per timepoint for 18 women with locally advanced cervical cancer treated with bone marrow sparing chemoradiotherapy with volumetric-modulated arc therapy. Datapoints left of the yellow horizontal line indicate grade ≥2 lymphopenia. The regression line, including the 95% confidence interval, R^2 and p-value, are also indicated. W = week, M = months.*

DISCUSSION

In this study, longitudinal changes in vertebral and pelvic bone marrow fat fraction and blood immune cell counts were evaluated in women with primary locally advanced cervical cancer undergoing bone marrow sparing chemoradiotherapy. A mean dose of 1–5 Gy caused an average increase of 23.8 PDFF% in vertebral PDFF, followed by an average decrease of 13.3 PDFF% at 3 months post-treatment. Interestingly, PDFF remained elevated compared to baseline up to 12 months after treatment. In vertebrae receiving >5 Gy, average PDFF increased with 34.7 PDFF% without recovery. A higher mean PDFF of the vertebral column resulted in a larger immunosuppressive effect, which lasted up to at least 12 months after treatment.

In this study, we analyzed a homogeneous patient cohort, used water-fat MRI that can detect differences >10 PDFF%, as differences <10 PDFF% were attributed to technical

variability in a validation study [36], and evaluated changes up to 12 months after treatment. The detected PDFF changes in vertebrae receiving no or a high dose are consistent with previous observations [26-29]. Our findings in the 1–5 Gy dose group suggested that doses around 5 Gy might be an important threshold for PDFF increase. McGuire et al. demonstrated a linear, negative relationship between the dose up to 6 Gy and bone marrow activity at one week post-treatment [38]. Our results further specified that bone marrow receiving a dose of 1–5 Gy shows some recovery in PDFF at 3 months after treatment, but that PDFF remains elevated compared to baseline even up to 12 months after treatment.

Bone marrow resident adipocytes were long considered as a filler of marrow space. However, multiple studies have demonstrated interactions, although contradictory, between bone marrow adipocytes and hematopoiesis [44]. Bone marrow adipocytes, on one hand, decrease the number and function of HSCs and worsen hematopoiesis [25, 45]. Mice incapable of forming adipocytes showed better hematopoietic recovery after irradiation and bone marrow transplantation than normal mice [25]. On the other hand, bone marrow adipocytes secrete factors and supply energy for HSC regeneration and hematopoiesis [21, 46, 47]. However, in irradiated mice, whether adipocytes promoted or inhibited hematopoiesis differed between bone marrow locations [21]. In our study, a higher mean PDFF of the vertebral column was associated with a decrease in circulating immune cells, highlighting the immunosuppressive effect of chemoradiotherapy, which lasted up to at least 12 months after treatment. As vertebral bone marrow receiving >5 Gy had a higher PDFF without recovery, reducing the amount of bone marrow receiving a high dose might reduce the immunosuppression caused by chemoradiotherapy. However, the complex interactions between bone marrow adipocytes and hematopoiesis ensure that the exact mechanisms remain an area of ongoing research.

Previous studies also demonstrated a positive correlation between age and bone marrow PDFF in healthy volunteers [48, 49] and after chemoradiotherapy [28]. Age-induced bone marrow fat increase is associated with an impaired function of HSCs, resulting in increased myelopoiesis and decreased lymphopoiesis [50-53]. In contrast, our study identified a positive association between age and the number of circulating lymphocytes and leukocytes, which was not detected for neutrophils. The exact interaction between age and bone marrow functioning in patients with cancer should therefore be further evaluated in future studies.

There might be heterogeneity in the activity and dose-response relationship with hematologic toxicity (HT) among bone marrow regions. Studies using functional imaging in the pelvic bones demonstrated that the lumbosacral region had the highest bone marrow activity [54, 55], which was stronger correlated to immune cell counts than for other bone marrow regions [56, 57]. Additionally, studies demonstrated a relationship between dose delivered to active bone marrow and the number of circulating immune cells [58-61]. However, dosimetric parameters correlating with HT were also identified for the whole pelvic bones and for each pelvic subregion [34, 62]. Despite our bone marrow sparing strategy, all women developed grade ≥2 lymphopenia. This result highlights that future studies determining the optimal bone marrow sparing strategy are warranted.

Since the majority of the patients completed four or more of the five planned chemotherapy cycles, we could not assess the impact of variations in chemotherapy exposure on PDFF or circulating immune cell counts. A previous study reported that lumbar vertebral PDFF increased by 25.7 PDFF% six months after myelotoxic chemotherapy, whereas it did not increase in the control group without chemotherapy [63]. Future studies could further investigate the impact of chemotherapy on longitudinal bone marrow PDFF changes and HT.

Our analysis was limited by the small number of vertebrae receiving a dose between 5 and 30 Gy, due to the steep dose-fall off in the vertebral column. Based on our data, 5 Gy could be an important dosimetric parameter. However, more data in the range between 5 and 30 Gy will be needed to validate this suggestion. As the VMAT technique used resulted in high dose levels and dose uniformity in the pelvic bones, with a mean dose of ≥18.8 Gy, with limited variability, with standard deviations between 7.9 and 64.8 cc on volumes between 234.5 and 408.1 cc for each subregion. Therefore, we cannot demonstrate an association between mean dose and PDFF in the pelvic bones, except for that of the ilium at 12 months post-treatment. Only the lower pelvis returned to its baseline PDFF level at 3 months after treatment, likely due to its initially high PDFF of 74% and low hematopoietic activity, which limits capacity for PDFF increase [27, 54]. However, similar to the other subregions, this recovery was not >10 PDFF%. Additionally, as PDFF does not assess bone marrow activity directly, it remains unclear if the lower pelvis functioning recovered. Future studies could explore the relationship between longitudinal PDFF changes and bone marrow functioning. A final limitation is that only dose to the pelvic and vertebral bone marrow was considered. Dose to lymphocyte-rich organs and a large irradiated (blood) volume are also associated with a higher risk of HT and should be

evaluated in future studies [64-69]. Because of the PROTECT study design, we included a relatively high number of patients undergoing para-aortic radiotherapy with large irradiated volumes, which might have impact on the number of vertebrae in each dose group and HT.

In conclusion, vertebral bone marrow proton density fat fraction (PDFF) increased at a mean dose >1 Gy, followed by a recovery when the mean dose was <5 Gy, and remained elevated up to 12 months post-treatment. In the pelvic bones, only the lower pelvic PDFF recovered to baseline level at 3 months post-treatment. The number of circulating immune cells was lower up to 12 months post-treatment, which was related to a higher mean vertebral PDFF. Bone marrow doses around 5 Gy could be a potential threshold for irreversible bone marrow damage, but this threshold should be validated in larger studies.

ACKNOWLEDGMENTS

We thank the patients and their families who participated in this study. We also would like to thank Hilde Roording, Britt Sticker, and Kiki van Duuren for developing the bone marrow delineation method and helping with bone marrow delineations.

SUPPLEMENTARY MATERIAL

Supplementary material is available on

REFERENCES

1. Huang J, Gu F, Ji T, Zhao J, Li G. Pelvic bone marrow sparing intensity modulated radiotherapy reduces the incidence of the hematologic toxicity of patients with cervical cancer receiving concurrent chemoradiotherapy: a single-center prospective randomized controlled trial. Radiation Oncology. 2020;15(1):180.
2. Albuquerque K, Giangreco D, Morrison C, Siddiqui M, Sinacore J, Potkul R, et al. Radiation-related predictors of hematologic toxicity after concurrent chemoradiation for cervical cancer and implications for bone marrow–sparing pelvic IMRT. International Journal of Radiation Oncology* Biology* Physics. 2011;79(4):1043-7.
3. Kumar T, Schernberg A, Busato F, Laurans M, Fumagalli I, Dumas I, et al. Correlation between pelvic bone marrow radiation dose and acute hematological toxicity in cervical cancer patients treated with concurrent chemoradiation. Cancer management and research. 2019:6285-97.
4. Williamson CW, Sirák I, Xu R, Portelance L, Wei L, Tarnawski R, et al. Positron emission tomography-guided bone marrow-sparing radiation therapy for locoregionally advanced cervix cancer: final results from the INTERTECC phase II/III trial. International Journal of Radiation Oncology* Biology* Physics. 2022;112(1):169-78.
5. Hara JH, Jutzy JM, Arya R, Kothari R, McCall AR, Howard AR, et al. Predictors of Acute Hematologic Toxicity in Women receiving extended-field chemoradiation for cervical Cancer: do known pelvic Radiation bone marrow constraints apply? Advances in Radiation Oncology. 2022;7(6):100998.
6. Wang SB, Liu JP, Lei KJ, Jia YM, Xu Y, Rong JF, et al. The volume of 99mTc sulfur colloid SPET- defined active bone marrow can predict grade 3 or higher acute hematologic toxicity in locally advanced cervical cancer patients who receive chemoradiotherapy. Cancer Medicine. 2019;8(17):7219-26.
7. Wang S, Liu J, Lei K, Jia Y, Wang C, Zhang X, et al. Single-photon emission computed tomography-defined active bone marrow-sparing volumetric-modulated arc therapy reduces the incidence of acute hematologic toxicity in locally advanced cervical cancer patients who receive chemoradiotherapy: A single-center prospective randomized controlled trial. Cancer. 2023;129(13):1995-2003.
8. Damen PJ, Kroese TE, van Hillegersberg R, Schuit E, Peters M, Verhoeff JJ, et al. The influence of severe radiation-induced lymphopenia on overall survival in solid tumors: a systematic review and meta-analysis. International Journal of Radiation Oncology* Biology* Physics. 2021;111(4):936-48.
9. Wu ES, Oduyebo T, Cobb LP, Cholakian D, Kong X, Fader AN, et al. Lymphopenia and its association with survival in patients with locally advanced cervical cancer. Gynecologic oncology. 2016;140(1):76-82.
10. Venkatesulu BP, Mallick S, Lin SH, Krishnan S. A systematic review of the influence of radiation-induced lymphopenia on survival outcomes in solid tumors. Critical Reviews in Oncology/Hematology. 2018;123:42-51.
11. Mellman I, Coukos G, Dranoff G. Cancer immunotherapy comes of age. Nature. 2011;480(7378):480-9.
12. Molon B, Calì B, Viola A. T Cells and Cancer: How Metabolism Shapes Immunity. Frontiers in Immunology. 2016;7.

13. Lorusso D, Xiang Y, Hasegawa K, Scambia G, Leiva M, Ramos-Elias P, et al. Pembrolizumab or placebo with chemoradiotherapy followed by pembrolizumab or placebo for newly diagnosed, high-risk, locally advanced cervical cancer (ENGOT-cx11/GOG-3047/KEYNOTE-A18): overall survival results from a randomised, double-blind, placebo-controlled, phase 3 trial. The Lancet. 2024;404(10460):1321-32.
14. Herter J, Kiljan M, Kunze S, Reinscheid M, Ibruli O, Cai J, et al. Influence of chemoradiation on the immune microenvironment of cervical cancer patients. Strahlentherapie und Onkologie. 2023;199(2):121-30.
15. Wang Y, Deng W, Li N, Neri S, Sharma A, Jiang W, et al. Combining immunotherapy and radiotherapy for cancer treatment: current challenges and future directions. Frontiers in pharmacology. 2018;9:185.
16. Holub K, Vargas A, Biete A. Radiation-induced lymphopenia: the main aspects to consider in immunotherapy trials for endometrial and cervical cancer patients. Clinical and Translational Oncology. 2020;22:2040-8.
17. Mauch P, Constine L, Greenberger J, Knospe W, Sullivan J, Liesveld JL, et al. Hematopoietic stem cell compartment: Acute and late effects of radiation therapy and chemotherapy. International Journal of Radiation Oncology*Biology*Physics. 1995;31(5):1319-39.
18. Ellis RE. The Distribution of Active Bone Marrow in the Adult. Physics in Medicine & Biology. 1961;5(3):255.
19. Shao L, Wang Y, Chang J, Luo Y, Meng A, Zhou D. Hematopoietic stem cell senescence and cancer therapy-induced long-term bone marrow injury. Transl Cancer Res. 2013;2(5):397-411.
20. Lichtman M. The ultrastructure of the hemopoietic environment of the marrow: a review. Experimental hematology. 1981;9(4):391-410.
21. Zhou BO, Yu H, Yue R, Zhao Z, Rios JJ, Naveiras O, et al. Bone marrow adipocytes promote the regeneration of stem cells and haematopoiesis by secreting SCF. Nature Cell Biology. 2017;19(8):891-903.
22. Green DE, Rubin CT. Consequences of irradiation on bone and marrow phenotypes, and its relation to disruption of hematopoietic precursors. Bone. 2014;63:87-94.
23. Zhang Y, Chen X, Wang X, Chen J, Du C, Wang J, et al. Insights into ionizing radiation-induced bone marrow hematopoietic stem cell injury. Stem Cell Research & Therapy. 2024;15(1):222.
24. Green DE, Adler BJ, Chan ME, Lennon JJ, Acerbo AS, Miller LM, et al. Altered composition of bone as triggered by irradiation facilitates the rapid erosion of the matrix by both cellular and physicochemical processes. PloS one. 2013;8(5):e64952.
25. Naveiras O, Nardi V, Wenzel PL, Hauschka PV, Fahey F, Daley GQ. Bone-marrow adipocytes as negative regulators of the haematopoietic microenvironment. Nature. 2009;460(7252):259-63.
26. Wang C, Qin X, Gong G, Wang L, Su Y, Yin Y. Correlation between changes of pelvic bone marrow fat content and hematological toxicity in concurrent chemoradiotherapy for cervical cancer. Radiation Oncology. 2022;17(1):70.
27. Bolan PJ, Arentsen L, Sueblinvong T, Zhang Y, Moeller S, Carter JS, et al. Water–fat MRI for assessing changes in bone marrow composition due to radiation and chemotherapy in gynecologic cancer patients. Journal of Magnetic Resonance Imaging. 2013;38(6):1578-84.

28. Carmona R, Pritz J, Bydder M, Gulaya S, Zhu H, Williamson CW, et al. Fat composition changes in bone marrow during chemotherapy and radiation therapy. International Journal of Radiation Oncology* Biology* Physics. 2014;90(1):155-63.
29. Qin X, Wang C, Gong G, Wang L, Su Y, Yin Y. Functional MRI radiomics-based assessment of pelvic bone marrow changes after concurrent chemoradiotherapy for cervical cancer. BMC Cancer. 2022;22(1):1149.
30. Wen X, Qin Q, Wu Y, Li Z, Yang X, Liu J, et al. Association between IDEAL-IQ MRI fat fraction quantification and pelvic bone marrow reserve function in concurrent chemoradiotherapy for cervical cancer. Radiation Medicine and Protection. 2023;4(3):136-44.
31. Corbeau A, Nout RA, Mens JWM, Horeweg N, Godart J, Kerkhof EM, et al. PROTECT: Prospective Phase-II-Trial Evaluating Adaptive Proton Therapy for Cervical Cancer to Reduce the Impact on Morbidity and the Immune System. Cancers. 2021;13(20):5179.
32. Pötter R, Tanderup K, Kirisits C, de Leeuw A, Kirchheiner K, Nout R, et al. The EMBRACE II study: The outcome and prospect of two decades of evolution within the GEC-ESTRO GYN working group and the EMBRACE studies. Clinical and translational radiation oncology. 2018;9:48-60.
33. Mell LK, Kochanski JD, Roeske JC, Haslam JJ, Mehta N, Yamada SD, et al. Dosimetric predictors of acute hematologic toxicity in cervical cancer patients treated with concurrent cisplatin and intensity-modulated pelvic radiotherapy. International Journal of Radiation Oncology*Biology*Physics. 2006;66(5):1356-65.
34. Corbeau A, Kuipers SC, de Boer SM, Horeweg N, Hoogeman MS, Godart J, et al. Correlations between bone marrow radiation dose and hematologic toxicity in locally advanced cervical cancer patients receiving chemoradiation with cisplatin: a systematic review. Radiotherapy and Oncology. 2021;164:128-37.
35. Kuipers S, Godart J, Corbeau A, Sharfo AW, Breedveld S, Mens JW, et al. The impact of bone marrow sparing on organs at risk dose for cervical cancer: a Pareto front analysis. Frontiers in Oncology. 2023;13.
36. Corbeau A, van Gastel P, Wielopolski PA, de Jong N, Creutzberg CL, van der Heide UA, et al. Accuracy, repeatability, and reproducibility of water-fat magnetic resonance imaging in a phantom and healthy volunteer. Physics and Imaging in Radiation Oncology. 2024;32:100651.
37. Health UDo, Services H. Common terminology criteria for adverse events (CTCAE) version 5.0. 2017.
38. McGuire SM, Bhatia SK, Sun W, Jacobson GM, Menda Y, Ponto LL, et al. Using [18F] Fluorothymidine Imaged With Positron Emission Tomography to Quantify and Reduce Hematologic Toxicity Due to Chemoradiation Therapy for Pelvic Cancer Patients. International Journal of Radiation Oncology*Biology*Physics. 2016;96(1):228-39.
39. McGuire SM, Menda Y, Ponto LLB, Gross B, Buatti J, Bayouth JE. 3'-deoxy-3'-[18F] fluorothymidine PET quantification of bone marrow response to radiation dose. International Journal of Radiation Oncology* Biology* Physics. 2011;81(3):888-93.
40. Schmeel FC, Vomweg T, Träber F, Gerhards A, Enkirch SJ, Faron A, et al. Proton density fat fraction MRI of vertebral bone marrow: Accuracy, repeatability, and reproducibility among readers, field strengths, and imaging platforms. Journal of Magnetic Resonance Imaging. 2019;50(6):1762-72.

41. Jang JK, Lee SS, Kim B, Cho E-S, Kim YJ, Byun JH, et al. Agreement and Reproducibility of Proton Density Fat Fraction Measurements Using Commercial MR Sequences Across Different Platforms: A Multivendor, Multi-Institutional Phantom Experiment. Investigative Radiology. 2019;54(8):517-23.
42. Baum T, Yap SP, Dieckmeyer M, Ruschke S, Eggers H, Kooijman H, et al. Assessment of whole spine vertebral bone marrow fat using chemical shift-encoding based water-fat MRI. Journal of Magnetic Resonance Imaging. 2015;42(4):1018-23.
43. Guerreiro F, van Houdt PJ, Navest RJM, Hoekstra N, de Jong M, Heijnen BJ, et al. Validation of quantitative magnetic resonance imaging techniques in head and neck healthy structures involved in the salivary and swallowing function: Accuracy and repeatability. Phys Imaging Radiat Oncol. 2024;31:100608.
44. Li Z, Rosen CJ. The Multifaceted Roles of Bone Marrow Adipocytes in Bone and Hematopoietic Homeostasis. The Journal of Clinical Endocrinology & Metabolism. 2023;108(12):e1465-e72.
45. Ambrosi TH, Scialdone A, Graja A, Gohlke S, Jank A-M, Bocian C, et al. Adipocyte accumulation in the bone marrow during obesity and aging impairs stem cell-based hematopoietic and bone regeneration. Cell stem cell. 2017;20(6):771-84. e6.
46. Li Z, Bowers E, Zhu J, Yu H, Hardij J, Bagchi DP, et al. Lipolysis of bone marrow adipocytes is required to fuel bone and the marrow niche during energy deficits. eLife. 2022;11:e78496.
47. Veldhuis-Vlug AG, Rosen CJ. Clinical implications of bone marrow adiposity. Journal of Internal Medicine. 2018;283(2):121-39.
48. Aoki T, Yamaguchi S, Kinoshita S, Hayashida Y, Korogi Y. Quantification of bone marrow fat content using iterative decomposition of water and fat with echo asymmetry and least-squares estimation (IDEAL): reproducibility, site variation and correlation with age and menopause. Br J Radiol. 2016;89(1065):20150538.
49. Baum T, Rohrmeier A, Syväri J, Diefenbach MN, Franz D, Dieckmeyer M, et al. Anatomical Variation of Age-Related Changes in Vertebral Bone Marrow Composition Using Chemical Shift Encoding-Based Water–Fat Magnetic Resonance Imaging. Frontiers in Endocrinology. 2018;9.
50. Linton PJ, Dorshkind K. Age-related changes in lymphocyte development and function. Nature Immunology. 2004;5(2):133-9.
51. Aaron N, Costa S, Rosen CJ, Qiang L. The Implications of Bone Marrow Adipose Tissue on Inflammaging. Front Endocrinol (Lausanne). 2022;13:853765.
52. Marinelli Busilacchi E, Morsia E, Poloni A. Bone Marrow Adipose Tissue. Cells. 2024;13(9):724.
53. Patel VS, Ete Chan M, Rubin J, Rubin CT. Marrow Adiposity and Hematopoiesis in Aging and Obesity: Exercise as an Intervention. Curr Osteoporos Rep. 2018;16(2):105-15.
54. McGuire SM, Menda Y, Ponto LLB, Gross B, TenNapel M, Smith BJ, et al. Spatial mapping of functional pelvic bone marrow using FLT PET. Journal of applied clinical medical physics. 2014;15(4):129-36.
55. Noticewala SS, Li N, Williamson CW, Hoh CK, Shen H, McHale MT, et al. Longitudinal Changes in Active Bone Marrow for Cervical Cancer Patients Treated With Concurrent Chemoradiation Therapy. International Journal of Radiation Oncology*Biology*Physics. 2017;97(4):797-805.

56. Yagi M, Froelich J, Arentsen L, Shanley R, Ghebre R, Yee D, et al. Longitudinal FDG-PET Revealed Regional Functional Heterogeneity of Bone Marrow, Site-Dependent Response to Treatment and Correlation with Hematological Parameters. J Cancer. 2015;6(6):531-7.

57. David JM, Yue Y, Blas K, Hendifar A, Kabolizadeh P, Tuli R. 18F-FDG PET Predicts Hematologic Toxicity in Patients with Locally Advanced Anal Cancer Treated With Chemoradiation. Advances in Radiation Oncology. 2019;4(4):613-22.

58. Elicin O, Callaway S, Prior JO, Bourhis J, Ozsahin M, Herrera FG. [18F]FDG-PET Standard Uptake Value as a Metabolic Predictor of Bone Marrow Response to Radiation: Impact on Acute and Late Hematological Toxicity in Cervical Cancer Patients Treated With Chemoradiation Therapy. International Journal of Radiation Oncology*Biology*Physics. 2014;90(5):1099-107.

59. Rose BS, Liang Y, Lau SK, Jensen LG, Yashar CM, Hoh CK, et al. Correlation Between Radiation Dose to 18F-FDG-PET Defined Active Bone Marrow Subregions and Acute Hematologic Toxicity in Cervical Cancer Patients Treated With Chemoradiotherapy. International Journal of Radiation Oncology*Biology*Physics. 2012;83(4):1185-91.

60. Yan K, Ramirez E, Xie X-J, Gu X, Xi Y, Albuquerque K. Predicting severe hematologic toxicity from extended-field chemoradiation of para-aortic nodal metastases from cervical cancer. Practical Radiation Oncology. 2018;8(1):13-9.

61. Zhou YM, Freese C, Meier T, Go D, Khullar K, Sudhoff M, et al. The absolute volume of PET-defined, active bone marrow spared predicts for high grade hematologic toxicity in cervical cancer patients undergoing chemoradiation. Clinical and Translational Oncology. 2018;20(6):713-8.

62. Konnerth D, Gaasch A, Zinn A, Rogowski P, Rottler M, Walter F, et al. Hematologic Toxicity and Bone Marrow-Sparing Strategies in Chemoradiation for Locally Advanced Cervical Cancer: A Systematic Review. Cancers. 2024;16(10):1842.

63. Gassert FG, Kranz J, Gassert FT, Schwaiger BJ, Bogner C, Makowski MR, et al. Longitudinal MR-based proton-density fat fraction (PDFF) and T2* for the assessment of associations between bone marrow changes and myelotoxic chemotherapy. European Radiology. 2024;34(4):2437-44.

64. Ellsworth SG. Field size effects on the risk and severity of treatment-induced lymphopenia in patients undergoing radiation therapy for solid tumors. Advances in Radiation Oncology. 2018;3(4):512-9.

65. Ellsworth SG, Yalamanchali A, Zhang H, Grossman SA, Hobbs R, Jin J-Y. Comprehensive analysis of the kinetics of radiation-induced lymphocyte loss in patients treated with external beam radiation therapy. Radiation research. 2020;193(1):73-81.

66. Tang C, Liao Z, Gomez D, Levy L, Zhuang Y, Gebremichael RA, et al. Lymphopenia Association With Gross Tumor Volume and Lung V5 and Its Effects on Non-Small Cell Lung Cancer Patient Outcomes. International Journal of Radiation Oncology*Biology*Physics. 2014;89(5):1084-91.

67. Fang P, Shiraishi Y, Verma V, Jiang W, Song J, Hobbs BP, et al. Lymphocyte-Sparing Effect of Proton Therapy in Patients with Esophageal Cancer Treated with Definitive Chemoradiation. International Journal of Particle Therapy. 2017;4(3):23-32.

68. Rudra S, Hui C, Rao YJ, Samson P, Lin AJ, Chang X, et al. Effect of Radiation Treatment Volume Reduction on Lymphopenia in Patients Receiving Chemoradiotherapy for Glioblastoma. International Journal of Radiation Oncology*Biology*Physics. 2018;101(1):217-25.

69. Venkatesulu B, Giridhar P, Pujari L, Chou B, Lee JH, Block AM, et al. Lymphocyte sparing normal tissue effects in the clinic (LymphoTEC): A systematic review of dose constraint considerations to mitigate radiation-related lymphopenia in the era of immunotherapy. Radiotherapy and Oncology. 2022;177:81-94.